Response to Reviewer #1

General comments:

Comment: *OVOCs play a central role in tropospheric radical chemistry by enhancing the atmospheric oxidizing capacity and promoting the formation of secondary pollutants. This manuscript investigates the role of primary OVOCs in ozone formation over the YRD region by implementing updated, source-resolved OVOC emission profiles into CMAQ and combining model evaluation with process-based and sensitivity analyses. The topic is timely and relevant to the ACP readership, given the growing attention to VOC/OVOC inventories, VCP-related emissions, and radical budgets in polluted regions. However, several issues need to be addressed before the manuscript can be considered for publication in ACP.*

Response: We thank the reviewer for the positive and constructive feedback on our study. The comments have been very helpful in improving the clarity and overall quality of the manuscript. In response to the reviewer's suggestions, we have: (1) clearly defined primary and secondary OVOCs and radical sources; (2) refocused the analysis on the role of OVOCs in primary radical production (HO_2, RO_2, and RO_x) to improve the mechanistic understanding of ozone formation; (3) quantitatively characterized the concentrations of key OVOCs and the associated model biases; (4) strengthened the evaluation of model performance in simulating organic acids and discussed the uncertainties related to their budgets and emission contributions; and (5) reorganized Section 3.1 to improve the overall structure of the manuscript. Detailed responses to each comment are provided below. The reviewer's comments are shown in black italics, our responses are in blue, and revisions in the manuscript are highlighted in red.

Specific comments

Comment: *1. Line 19, The original statement "The model well captured the diurnal and seasonal variations of most OVOCs". Please clarify whether the model captures the variations in OVOC emission fluxes or in OVOC concentrations. In addition, support the statement more quantitatively (e.g. by quoting ranges of R, NMB, NME for key OVOC classes) rather than relying mainly on qualitative descriptions.*

Response: Thank you for pointing out this ambiguity. In Lines 19-21, we have revised it to: "The model reproduced the diurnal and seasonal variations of most observed OVOC concentrations, particularly carbonyl compounds, with moderate correlation coefficients of 0.40−0.79."

Comment: *2. Throughout the paper, "primary OVOCs", "emitted OVOCs" and "directly emitted OVOCs" are used. For clarity and consistency (also with the paper title), I recommend adopting "primary OVOCs" as the main term and defining it*

explicitly in Sect. 2 (e.g. primary = directly emitted from anthropogenic/biogenic sources; secondary = produced via VOC oxidation). Please ensure that the terminology is used consistently in the text, figures, and captions.

Response: We fully agree with your suggestion. To ensure consistency throughout the text, we have revised terminology, such as "emitted OVOCs" and "directly emitted OVOCs", to "primary OVOCs". Additionally, we have added a clear definition of primary and secondary OVOCs in Section 2.1, in Lines 143-145:

"In this study, primary OVOCs are defined as those directly emitted from anthropogenic and biogenic sources, whereas secondary OVOCs refer to those formed via the photooxidation of VOC precursors."

Furthermore, we have reviewed and revised all figure and table captions to ensure terminology consistency.

Comment: *3. Section 3.1, This section currently mixes the description of observed OVOC concentration characteristics with the discussion of model simulation results, which makes the content rather long and somewhat fragmented. I suggest splitting it into two subsections, separating the presentation of observations from the evaluation of model performance.*

Response: Thank you for the valuable suggestion, which has helped improve the clarity and organization of the manuscript. In the original manuscript, observations and model results were discussed together by species to facilitate a focused interpretation of OVOC characteristics and the associated model biases. To enhance readability and better align with your recommendation, we have reorganized this part of the manuscript by separating model evaluation from the regional analysis. Specifically, the original section has been divided into two subsections: Section 3.1, "Model evaluation", which emphasizes the evaluation of model performance while describing key observational features at the monitoring site; and Section 3.2, "Regional characteristics of OVOCs", which presents the simulated OVOC distributions and source contributions across the YRD region during the two episodes (EP1 and EP2). The section numbering in the remainder of the manuscript has been updated accordingly.

Comment: *4. Section 3.1, For some species (e.g. acids, alcohol) the discussion emphasizes underestimation or overestimation, but quantitative information on observed mean/median concentrations is limited. It would be helpful to briefly summarize typical concentration ranges for the main OVOC classes in the main text or in a supplementary table, to give readers a clearer sense of magnitude.*

Response: Thank you for the valuable suggestion. The mean observed and predicted OVOC concentrations at the monitoring site have been included in the original Table S5. To ensure the representativeness of the results, CIIE-period (temporary emission

control measures during the China International Import Expo 2019) data were excluded, thereby avoiding model discrepancies caused by temporary emission regulations and accurately reflecting typical emission scenarios. We have also included descriptions of OVOC concentrations at the monitoring site in the revised text as follows:

Lines 183-185: "Among all the observed OVOCs, alcohols emerged as the dominant species in spring (EP1), with ethanol exhibiting the highest median concentrations (6−12 ppb), which declined to 1.9−4.6 ppb in fall (EP2)."

Lines 196-197: "Formic acid and acetic acid were the most abundant organic acids during both episodes, with the average concentrations of 0.15 (1.95) ppb and 1.88 (2.59) ppb in the EP1 (EP2) period, respectively."

Lines 227-229: "HCHO and acetone (ACET) were the most abundant aldehyde and ketone species, with average observed concentrations of 2.52 (2.58) ppb and 5.75 (1.89) ppb during EP1 (EP2), respectively."

Lines 249-251: "HCHO, MEOH, ACET, and acetaldehyde (CCHO) were the dominant species (Fig. S8), with concentration ranges of 2−8 ppb, 2−4 ppb, 2−4 ppb, and 1−3 ppb, respectively."

Lines 254-256: "The concentrations of ETOH, HCOOH, and CCOOH fell in ranges of 1.0–3.0 ppb, 0.1–0.4 ppb, and 0.5–2.0 ppb, respectively. Given the substantial underestimations of all three species, their actual concentrations are likely higher than the model predictions."

Comment: *5. Lines 213-215: Is there any evidence or supporting analysis to substantiate the conclusion that the biogenic contribution is higher during the warm season?*

Response: We have included a regional distribution of the average MEOH emission rates and contributions from biogenic sources across the YRD region in EP1 and EP2 in the supplement Fig. S9 (as shown below). The emission rates of MEOH are much higher during EP1 than during EP2. The main text has been revised accordingly as follows:

Lines 251-253: "High levels of HCHO, ACET, and CCHO mainly occurred in areas strongly influenced by anthropogenic emissions, where MEOH was predominantly concentrated in regions affected by biogenic emissions in the southern and southwestern YRD (Fig. S9)."

Lines 258-260: "The higher simulated MEOH concentrations in EP1 relative to EP2 may be partially attributed to stronger contributions from biogenic sources during the warm season (Fig. S9d, h)."

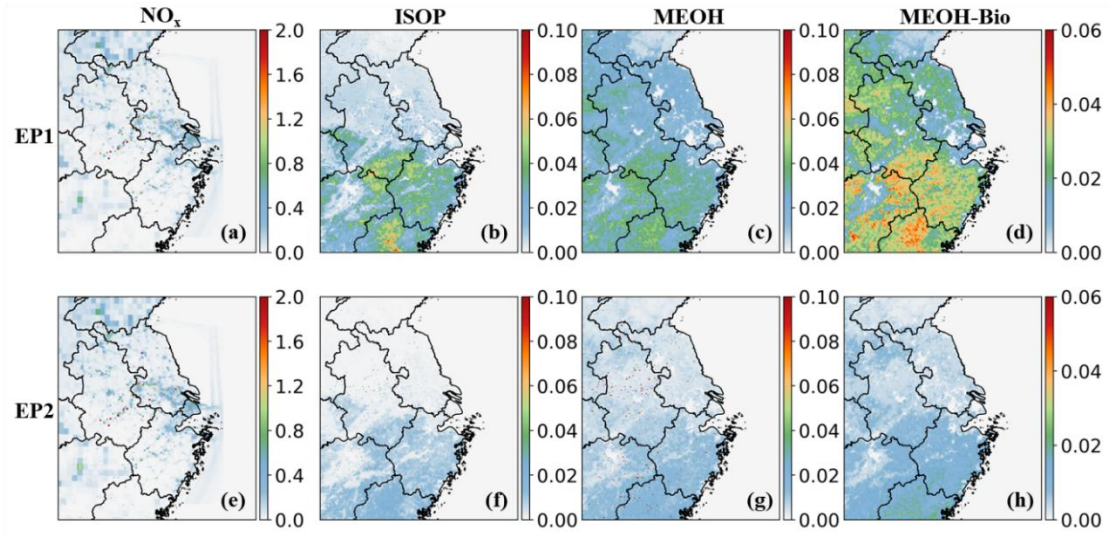

Figure S9. Average emission rates of NO_x, isoprene, MEOH, and biogenic MEOH during EP1 and EP2. Units are mole s^{-1}.

Comment: *6. Section 3.2, The authors acknowledge missing or simplified pathways for the production and loss of small aldehydes and organic acids. Given the importance of these processes for formic and acetic acid biases, please expand slightly on which multiphase/heterogeneous reactions are included (e.g. glyoxal/methylglyoxal uptake, aqueous-phase oxidation) and which are missing, and discuss how these omissions could affect both OVOC budgets and the derived role of primary emissions.*

Response: Thank you for the insightful comment. In the current model, heterogeneous losses of glyoxal and methylglyoxal are parameterized by first-order reactions, with the rates determined by uptake coefficients (γ). We adopt the values of γ reported by Everns and Volkamer (2010), 0.016 during daytime and a constant loss rate of 3.33×10^{-4} s^{-1} at night, which have been applied in our previous work and described in the original manuscript in lines 87-89:

"Several model updates, including heterogeneous reactions of sulfur dioxide (SO_2), NO_2, glyoxal, and methylglyoxal, were implemented as described in a previous study (Mao et al., 2022)."

However, the uptake of these dicarbonyl species is affected by their interactions with inorganic aerosols, known as "salting effects", which is not considered in the current model. Once uptake into the aqueous phase of aerosols, both dicarbonyls can be oxidized to produce formic and acetic acids (and other products) through complex reactions. These processes are poorly represented in most commonly used chemical transport models, including CMAQ, with all the products lumped into a surrogate species. The simplified treatment of the heterogeneous chemistry of these dicarbonyl species could partially explain the underestimation of methylglyoxal, formic acid, and acetic acid. We have clarified this in the revised manuscript in Lines 208-219:

"Therefore, the underestimation of both formic and acetic acids may partially stem from insufficient representation of secondary production. Observations showed that formic acid exhibited moderate to strong correlations with its precursor methylglyoxal in both periods. Laboratory studies have demonstrated that both formic and acetic acids can be produced via aqueous-phase reactions of glyoxal and methylglyoxal (Yu et al., 2011; Zhang et al., 2021; Sui et al., 2017; Lim et al., 2013), with uptake modulated by interactions with inorganic aerosols (i.e., salting effects) (Waxman et al., 2015; Kampf et al., 2013). In the current model, these heterogeneous processes are represented by first-order reactions, with rate constants determined by fixed uptake coefficients (γ=0.016 during daytime and a constant loss rate of 3.33×10^{-4} s^{-1} at night), and all products are lumped into a single surrogate species. The simplified treatment of heterogeneous chemistry likely leads to an underestimation of formic and acetic acids, particularly under high aerosol loadings in urban environments, where salting-out effects reduce their solubility in the aqueous phase (Babaei-Gharehbagh et al., 2025)."

Other secondary production of formic and acetic acids, such as multiphase reactions of HCHO (to produce formic acid), photochemical aging of aerosols, are not included in the current model. In addition, the yield of formic and acetic acids from precursor VOCs may be underestimated and contribute to the model biases of these organic acids. This has been clarified in the revised manuscript in Lines 219-223:
"Other sources of model bias may include missing secondary formation pathways, such as multiphase reactions of HCHO and photochemical aging of aerosols, and underestimated yields of formic and acetic acids from precursor VOCs (Yuan et al., 2015; Millet et al., 2015; Permar et al., 2023; Jiang et al., 2023; Cope et al., 2021; Franco et al., 2021; Malecha and Nizkorodov, 2016; Shen et al., 2026)."

Inadequate representation of secondary production may lead to an overestimation of emission contributions to formic and acetic acids. However, the discrepancies between the model and observations may also partially arise from underestimated emissions of these two species. As a result, the combined effects of these factors make it difficult to quantitatively assess the contributions of emissions to their concentrations. We have added discussions in the revised manuscript to address the potential impacts on their budgets and the associated emission contributions, as detailed below:
Lines 274-276: "Notably, the emission contributions of CCOOH may be biased due to uncertainties in emission inventories and chemical production in the model."

Comment: *7. Section 3.2, The terminology for HO2 sources (primary from VOC/OVOC oxidation, "newly generated" from photolysis and O_3 reactions, etc.) is central to the conclusions. I recommend adding a concise schematic or a table defining each category before Fig. 3 and clarifying whether "primary" HO2 excludes contributions from RO2 to HO2 recycling. This will help readers interpret Fig. 3c-e and the subsequent regional analysis.*

Response: Thank you for this constructive comment. Because HO_2, RO_2, and OH radicals are closely coupled and undergo rapid interconversion, the revised manuscript focuses on the production of primary (newly generated) radicals formed directly via photolysis (OVOCs, HONO, and O_3) and ozonolysis (OVOCs and unsaturated VOCs) reactions, in which radicals are generated solely as reaction products. Contributions from radical interconversion and cycling are therefore not included. Primary radicals initiate atmospheric radical chemistry and trigger radical chain reactions, ultimately leading to ozone accumulation. By focusing on the contribution of OVOCs to primary radical production, we provide a clearer and more robust assessment of their role in ozone formation. The manuscript has been revised accordingly to include a discussion of primary radical production from OVOCs in Section 3.3. Accordingly, a definition of primary radicals has been added to the revised manuscript, as described below:

Lines 323-327: "To elucidate the mechanism of daytime HO_2 radical production, the contributions of OVOCs to the formation of primary HO_2, RO_2, and RO_x radicals (RO_x = HO_2 + OH + RO_2) are assessed. Primary radicals refer to those generated through the photolysis of OVOCs, nitrous acid (HONO), and O_3 and the ozonolysis of OVOCs and unsaturated VOCs, while contributions from radical interconversion and cycling are excluded."

Technical comments

Comment: *1. Lines 41-43, please insert relevant reference for the box models results.*

Response: References on box model studies have been added in Line 45.

Comment: *2. Line 149, I suggest adding the word "concentration" to the section title to more clearly reflect the main focus of this subsection.*

Response: Thank you for the comment. To improve the clarity and overall organization of the manuscript, as suggested by the reviewer, the original section has been divided into two separate sections: "Model evaluation" and "Regional characteristics of OVOCs".

Response to Reviewer #2

Comment: *The manuscript entitled "Impact of Primarily Emitted Oxygenated Volatile Organic Compounds (OVOCs) on Ozone Formation in the Yangtze River Delta Region" presents a timely and valuable contribution to understanding the role of OVOCs in radical chemistry and ozone production. By integrating source-resolved OVOC emission profiles into the CMAQ model and evaluating them against observations during two typical pollution episodes, the study provides new insights into the contributions of primary OVOCs to HO_2 production and O_3 formation. Overall, the manuscript is well structured, the topic is highly relevant to ACP, and the results are scientifically meaningful. The use of source-resolved emission profiles and process-based analysis represents a methodological advancement with clear implications for regional air quality management. I believe the study has strong potential for publication after revisions. The specific comments are as follows.*

Response: We thank the reviewer for the positive and constructive feedback on our study. The comments have greatly helped improve the clarity and overall quality of the manuscript. In response to the reviewer's suggestions, we have: (1) explicitly articulated the scientific gaps addressed by this study; (2) elaborated on the methodology and uncertainties associated with the emission profiles; (3) refined the description of observational data processing; and (4) clarified concepts related to radical chemistry. Detailed responses to each comment are provided below. The reviewer's comments are shown in black italics, our responses are in blue, and revisions in the manuscript are highlighted in red.

Comment: *1. While the Introduction section provides a comprehensive overview of OVOC chemistry, emission uncertainties, and model limitations, the scientific gap addressed by the present study is not explicitly articulated. The manuscript would benefit from clearly stating (1) what aspects of primary OVOC contributions to HO_2 and O_3 formation remain unresolved in current literature. (2) How existing CTM/box model approaches fall short in quantifying emitted vs. secondary OVOC pathways. (3) Why a sector-resolved emission inventory is essential for addressing these limitations. More explicit formulation of these open questions at the end of the Introduction would help readers better understand the novelty and motivation of the study.*

Response: Thank you for this valuable comment. To emphasize the gaps in quantitatively assessing the contributions of primary emissions to OVOC concentrations and influences in radical chemistry and ozone formation, the introduction has been revised as follows:

Lines 73-85: "In this study, an updated emission inventory with refined profiles of OVOCs and their VOC precursors is incorporated into the Community Multiscale Air

Quality (CMAQ) model to improve OVOC simulations over the Yangtze River Delta (YRD) region in China. Our previous work demonstrated the critical role of OVOC oxidation in enhancing atmospheric oxidation capacity and promoting ozone formation in this region, based on top-down emission adjustments constrained by field observations (Li et al., 2022a). To build upon those findings, we employ a speciation-improved bottom-up approach by integrating updated sector-specific source profiles into the YRD emission inventory, thereby refining the speciation of primary OVOCs and quantifying the contributions of their precursors. Based on this refinement, the roles of primary and secondary OVOCs in radical production and ozone formation, as well as the significance of primary OVOCs and traditional VOC precursors on ozone mitigation during a pollution episode, are investigated. These findings help bridge the knowledge gap regarding the complex sources and atmospheric evolution of OVOCs, elucidating their crucial roles in influencing urban ozone chemistry."

Comment: *2. The updated 2019 YRD emission inventory incorporates extensive source-resolved OVOC profiles, which is a major strength of the study. However, the methodology would benefit from a more explicit discussion of the uncertainties associated with these refinements. For example, it is not entirely clear how the 160 localized measurements and literature-based profiles were weighted or harmonized across sectors, and whether any sensitivity tests were performed to evaluate the impact of these updates on simulated OVOC concentrations.*

Response: Thank you for the insightful suggestion. In the revised manuscript, we have clarified the methodology for developing the source profiles. Specifically, our approach follows the Technical Guidelines for Compiling Integrated Emission Inventories of Air Pollutants and Greenhouse Gases (Ministry of Ecology and Environment, 2024). After sampling and data collection, the profile of each source category was developed through a two-step process:

(1) Sub-category Averaging: To minimize the influence of individual sample variability, measurements were averaged to derive stable, representative profiles for each sub-category. For example, diesel vehicle emissions were classified according to China VI, China V, and China IV emission standards, respectively. For industrial processes, representative profiles were derived according to specific industrial stages, raw materials, products, and fuel types. Similarly, for biomass burning emissions, fuel-specific profiles were established.

(2) Weighted Integration: The final integrated source profiles were synthesized by weighting the sub-category profiles according to their respective total VOC emission contributions in the study region.

We have revised the manuscript to reflect these details in Lines 116-134 as follows:

"The VOC composition of emissions from diesel vehicles, industrial processes, and residential biomass burning was characterized based on 160 localized, source-resolved measurements conducted in China. Specifically, twenty in-use heavy-duty diesel vehicles from five major brands were tested, encompassing China VI (n=6), China V (n=10), and China IV (n=4) emission standards. For industrial emissions, a total of 84 samples were collected from priority sectors, including petrochemical industries, chemical raw material production, and other chemical production sectors such as plywood production, coking, pesticides production, ink production, and rubber production. For residential biomass burning, 23 samples of the combustion of four representative biomass fuels (wood, corncob, bean straw, and corn straw) and two common coal types (anthracite and briquette coal) were collected from the stack nozzles of household stoves. Details of the sampling protocols and analytical procedures can be found in a previous study (Gao et al., 2023). VOC profiles for other sources, such as gasoline vehicles, were based on published literature (Wang et al., 2022a; Huang et al., 2024). To develop representative source profiles, a two-step aggregation method was employed. First, sub-category average profiles were derived by averaging individual samples within each specific emission standard, industrial stage, and types of raw materials, products, and fuels. Second, the integrated source profiles were synthesized by weighting these sub-category profiles according to their corresponding total VOC emissions. This method aligns with the national technical guidelines for integrated air pollutant emission inventories (Ministry of Ecology and Environment, 2024)."

Comment: *3. The description of observational data is generally clear, but the treatment of PTR-QiTOF measurements requires slightly more detail. In particular, clarification on how fragmentation of alcohols was handled, how specific OVOC species were isolated from total protonated ion signals, and whether cross-validation with GC-MS was performed would enhance methodological transparency.*

Response: Thank you for this valuable suggestion. For most target OVOCs (such as aldehydes, ketones, and acids) measured by PTR-QiTOF, the molecular formula for individual mass spectral peaks was first constrained by jointly applying the elemental composition tool implemented in the Tofware software package v3.2.3 (Tofwerk Inc.), the PTR-MS spectral library (Pagonis et al., 2019), and the PubChem database. Based on these plausible molecular formulae, tentative compound identifications were further inferred by integrating previously reported source-specific emission profiles from the literature.

For species quantification, sensitivities for species with authentic standards were determined through calibration using multi-gradient known concentrations of given VOCs. For identified species lacking standards, their theoretical sensitivities were

estimated based on the correlations with kinetic rate constants of VOCs (Sekimoto et al., 2017). This approach has been successfully employed to identify reactive organic gases emitted from residential combustion in the YRD (Gao et al., 2022; 2023).

In the current study, small alcohols such as methanol and ethanol were detected using an online gas chromatography system equipped with a mass spectrometer and a flame ionization detector (GC-MS/FID). The results for major aromatic hydrocarbons and carbonyl compounds measured by PTR-QiTOF and GC-MS/FID show good agreement, as illustrated in Fig. S5 of Gao et al (2022).

We have revised the manuscript with detailed information on the treatment of PTR-QiTOF measurements and comparison between PTR-QiTOF and GC-MS/FID as follows:

Lines 148-160: "High time-resolution measurements of 77 OVOCs, including 14 aldehydes and ketones, 23 organic acids and esters, 10 furan compounds, and 30 oxygenated aromatic compounds, were recorded at a 10s interval using a Proton Transfer Reaction-Quadruple interface Time-of-Flight Mass Spectrometer (PTR-QiTOF) at the Shanghai Academy of Environmental Sciences (SAES). Species were identified by jointly applying the Tofware software package v3.2.3 (Tofwerk Inc.), the proton transfer reaction mass spectrometry (PTR-MS) spectral library (Pagonis et al., 2019), the PubChem database, and source-specific emission profiles reported in literature (Hatch et al., 2017; Koss et al., 2018; Stockwell et al., 2021; Tanzer-Gruener et al., 2022; Coggon et al., 2021). Sensitivities for species with authentic standards were determined through calibration using multi-gradient known concentrations of given VOCs. For identified species lacking standards, their theoretical sensitivities were estimated based on correlations with kinetic rate constants of VOCs (Sekimoto et al., 2017). The raw data were screened to remove outliers (values below background levels) and missing data, and then averaged to hourly means."

Lines 161-165: "In addition, C_2–C_{12} hydrocarbons, C_2–C_5 carbonyls, and C_1–C_4 alcohols were measured using an online gas chromatography system equipped with a mass spectrometer and a flame ionization detector (GC-MS/FID, TH-300, Wuhan Tianhong Instruments, China) at an hourly resolution. For major aromatic hydrocarbons and carbonyl compounds, good agreement between measurements by PTR-QiTOF and GC-MS/FID was observed (Gao et al., 2022)."

Comment: *4. This manuscript repeatedly distinguishes among "primary HO2," "newly generated HO2," and HO2 derived from OVOC_pri, OVOC_sec, and RO_2 pathways. However, the conceptual boundaries among these categories remain*

somewhat unclear, especially regarding whether RO_2-to-HO_2 conversions are counted as primary or secondary production. I recommend adding a concise schematic or a table summarizing the definitions and accounting logic to help readers interpret Figs. 3c–e more clearly.

Response: Thank you for this insightful comment. We agree with the reviewer that the production pathways of HO_2 radicals were not clearly defined in the original manuscript. Given the strong coupling and rapid interconversion among HO_2, RO_2, and OH radicals, we now focus exclusively on primary radical production, defined here as radicals generated directly as products of the photolysis of OVOCs, O_3, and HONO, as well as the ozonolysis of OVOCs and unsaturated VOCs. Contributions from radical interconversion and cycling are therefore excluded. Primary radicals initiate atmospheric radical chemistry and trigger radical chain reactions, ultimately leading to ozone accumulation. By focusing on the contribution of OVOCs to primary radical production, we provide a clearer and more robust assessment of their role in ozone formation. The results indicate that OVOCs make substantial contributions to both HO_2 and RO_2 production, accounting for more than 90% of primary HO_2 production and 50−90% of primary RO_2 production. Although secondary OVOCs exert a more pronounced influence on primary peroxy radical production at the regional scale, primary OVOCs can contribute up to 50% of primary peroxy radical production in areas with substantial OVOC emissions. Given that HO_2 radicals are a key driver of NO-to-NO_2 conversion in regions strongly influenced by anthropogenic emissions, OVOCs, particularly primary OVOCs, play an important role in urban ozone production. The manuscript has been revised to include a discussion of primary radical production from OVOCs in Section 3.2 (now Section 3.3). A definition of primary radicals has been added in the revised manuscript, as follows:

Lines 323-327: "To elucidate the mechanism of daytime HO_2 radical production, the contributions of OVOCs to the formation of primary HO_2, RO_2, and RO_x radicals (RO_x = HO_2 + OH + RO_2) are assessed. Primary radicals refer to those generated through the photolysis of OVOCs, nitrous acid (HONO), and O_3 and the ozonolysis of OVOCs and unsaturated VOCs, while contributions from radical interconversion and cycling are excluded."

Comment: *5. The description of ozone changes (ΔO3) would benefit from clearer definition. It is currently unclear whether the reported values (e.g., 0.90 ppb for HCHO) refer to domain-averaged responses, grid-level maxima, Shanghai city averages, or daytime peak ozone. Explicitly defining the metric, averaging period, and spatial domain would greatly improve interpretability and comparability of the sensitivity results.*

Response: Thank you for pointing out this ambiguity. We have clarified this at the

beginning of Section 3.3 (now Section 3.4) in Lines 383-384:
"The daytime average ozone responses to the complete removal of various VOCs (ΔO_3) at SAES".

References

Gao, Y., Wang, H., Yuan, L., Jing, S., Yuan, B., Shen, G., Zhu, L., Koss, A., Li, Y., Wang, Q., Huang, D. D., Zhu, S., Tao, S., Lou, S., and Huang, C.: Measurement report: Underestimated reactive organic gases from residential combustion – insights from a near-complete speciation, Atmos. Chem. Phys., 23, 6633-6646, 10.5194/acp-23-6633-2023, 2023.

Gao, Y. Q., Wang, H. L., Liu, Y., Zhang, X., Jing, S. A., Peng, Y. R., Huang, D. D., Li, X., Chen, S. Y., Lou, S. R., Li, Y. J., and Huang, C.: Unexpected High Contribution of Residential Biomass Burning to Non-Methane Organic Gases (NMOGs) in the Yangtze River Delta Region of China, J. Geophys. Res. Atmos., 127, 14, 10.1029/2021jd035050, 2022.

Ministry of Ecology and Environment, P. R. of C.: Technical Guidelines for Compiling an Integrated Emission Inventory of Air Pollutants and Greenhouse Gases, available at: https://www.mee.gov.cn/xxgk2018/xxgk/xxgk2006/202401/t20240130_21065242.html, 2024.

Pagonis, D., Sekimoto, K., and de Gouw, J.: A Library of Proton-Transfer Reactions of H3O+ Ions Used for Trace Gas Detection, Journal of the American Society for Mass Spectrometry, 30, 1330-1335, 10.1007/s13361-019-02209-3, 2019.

Sekimoto, K., Li, S.-M., Yuan, B., Koss, A., Coggon, M., Warneke, C., and de Gouw, J.: Calculation of the sensitivity of proton-transfer-reaction mass spectrometry (PTR-MS) for organic trace gases using molecular properties, International Journal of Mass Spectrometry, 421, 71-94, https://doi.org/10.1016/j.ijms.2017.04.006, 2017.

Response to Reviewer #3

Comment: *This study focuses on the impact of primarily emitted oxygenated volatile organic compounds (OVOCs) on ozone formation in the Yangtze River Delta region. By integrating an updated anthropogenic emission inventory with source-resolved profiles and the CMAQ model, it optimizes the simulation of OVOCs in the region. Combined with observational data from spring and autumn 2019, the study systematically analyzes the spatiotemporal distribution, source characteristics of OVOCs and their role in the ozone formation chain. The research is solid with sufficient data support, filling the research gap in the region and providing important scientific basis for targeted ozone pollution control with clear practical guiding significance. While the paper demonstrates a clear structure and standardized methods that meet journal publication requirements, it requires further revisions before being recommended for acceptance.*

Response: We sincerely thank the reviewer for the positive and constructive feedback on our study. These comments have substantially improved the clarity, rigor, and overall quality of the manuscript. In response to the reviewer's suggestions, we have: (1) added sensitivity simulations for primary OVOCs emitted from industrial processes, solvent use, transportation, and residential sources to quantify their impacts on ozone production rates as well as HO_2 and RO_2 radical concentrations; (2) conducted additional simulations incorporating temperature-dependent adjustments of evaporative emissions to assess the influences on OVOC levels; (3) quantified the contributions of OVOCs to primary HO_2, RO_2, and RO_x production; (4) elaborated on the heterogeneous and nonlinear responses of ozone to changes in OVOC emissions; (5) refined the description of observational data processing; and (6) made revisions to improve the clarity of the text and to standardize the fonts in all figures. Detailed responses to each comment are provided below. The reviewer's comments are shown in black italics, our responses are provided in blue, and the corresponding revisions in the manuscript are highlighted in red.

General Comments:

Comment: *It is recommended that the authors strengthen the analysis of the synergistic effects between primary OVOC emissions and other key pollutants (e.g., NO_x, CO, and traditional VOCs) across different source sectors. The study has well quantified the individual contributions of OVOCs to ozone formation, but it lacks in-depth discussion on how the interactions between OVOCs from specific sources (e.g., industrial processes, solvent use, and transportation) and other pollutants regulate the radical budget (especially HO_2 and RO_2) and ozone production efficiency. For instance, the differential impacts of OVOC-sourced HO_2 radicals on NO-to-NO_2 conversion under*

varying NO_x levels (high-NO_x urban areas vs. low-NO_x suburban areas) are not fully elaborated. It is suggested to supplement comparative analysis of such synergistic mechanisms, combined with source-resolved sensitivity simulations, to clarify the context-dependent roles of primary OVOCs in ozone formation, thereby enhancing the practical relevance for targeted emission control strategies.

Response: Thank you for the insightful suggestions. We have conducted four additional sensitivity simulations to assess the impacts of primary OVOCs emitted from industrial processes, solvent use, transportation, and residential sources in the YRD region on daytime peroxy radical (HO_2 and RO_2) concentrations and ozone production rates ($P(O_3)$) (Figs. R1-R4). In these simulations, OVOC emissions from each source category were individually set to zero. Among these sources, industrial processes showed the strongest impacts in Jiangsu Province, contributing up to 4 ppb h^{-1} of $P(O_3)$ and more than 1 ppt to HO_2 and RO_2 concentrations. The impacts of solvent use were mainly concentrated in the adjacent areas of Shanghai, Jiangsu, and Zhejiang, contributing up to 1 ppb h^{-1} to $P(O_3)$ and up to 36.8% of HO_2 and 46.8% of RO_2 radicals. For residential sources, the impacts on $P(O_3)$ were mainly concentrated in the central and northern YRD, with a hotspot over Shanghai reaching more than 0.1 ppb h^{-1}. In contrast, their influence on peroxy radicals was more spatially widespread across the YRD, contributing up to 2% of HO_2 and 3% of RO_2. Transportation sources exhibited relatively small but spatially widespread impacts on $P(O_3)$ as well as on HO_2 and RO_2, contributing up to 5.2%, 5.7%, and 4.0%, respectively. Overall, all these source categories except residential sources showed stronger impacts on HO_2 than RO_2 in regions strongly affected by anthropogenic emissions, highlighting the important role of primary OVOCs in ozone formation via the HO_2 + NO pathway.

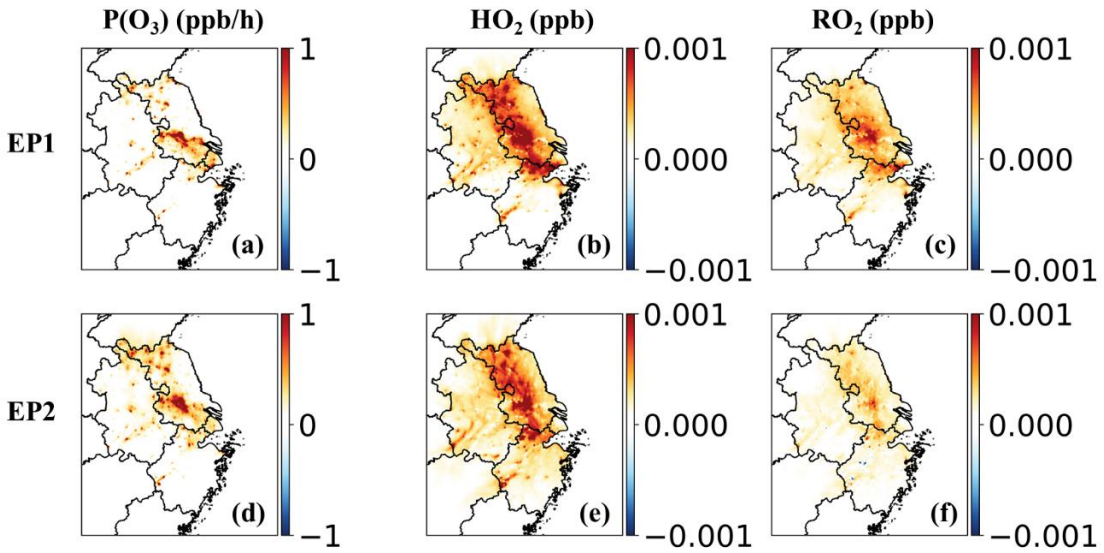

Figure R1. Contributions of OVOCs emitted from industrial processes to the daytime ozone production rate ($P(O_3)$, ppb h^{-1}) and HO_2 and RO_2 radical concentrations (ppb) during EP1 and EP2. The contributions are quantified as the differences between the base case and a sensitivity case in which

OVOC emissions from the corresponding sources are set to zero.

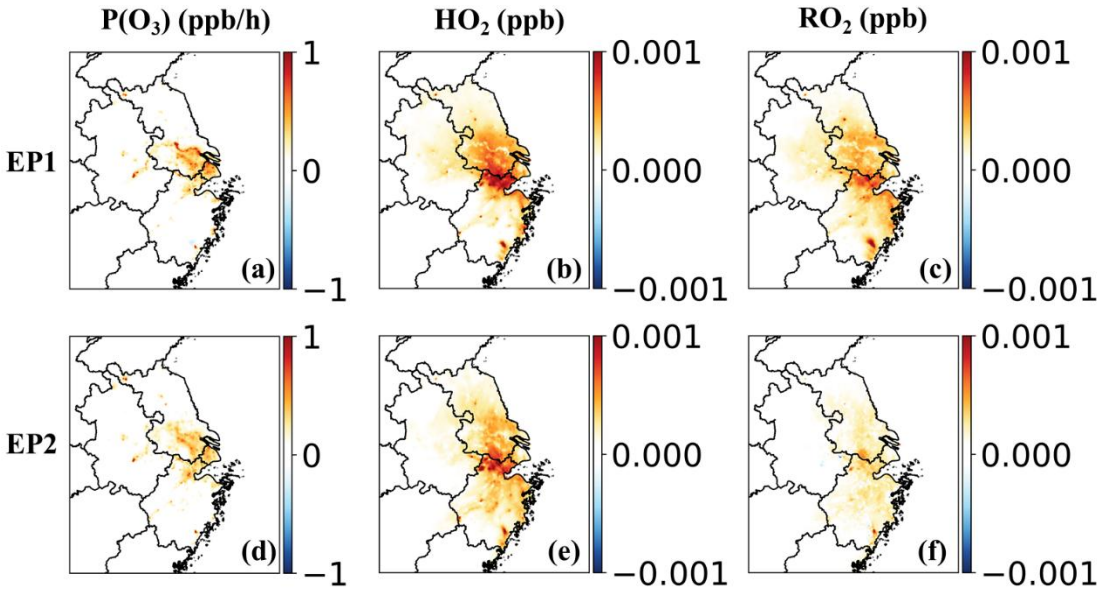

Figure R2. Same as Figure R1 but for the impacts of OVOCs emitted from solvent use sources.

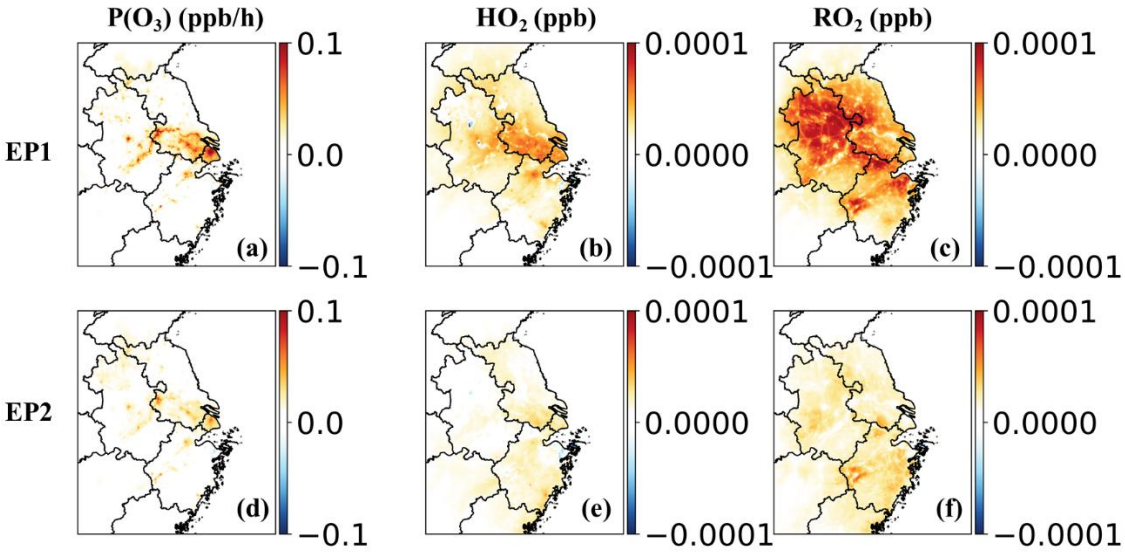

Figure R3. Same as Figure R1 but for the impacts of OVOCs emitted from residential sources.

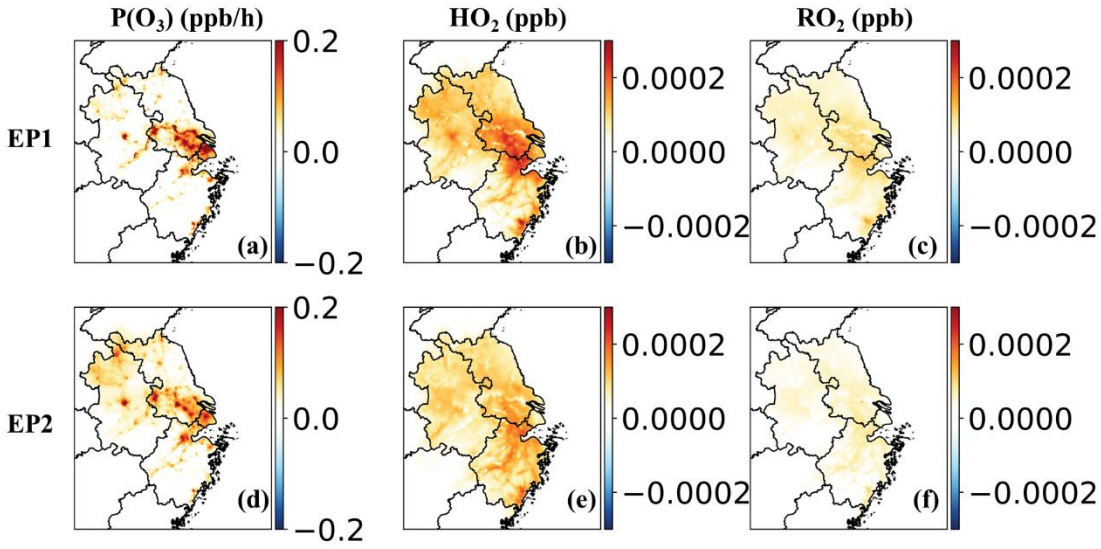

Figure R4. Same as Fig. R1 but for the impacts of OVOCs emitted from transportation sources.

Based on the daytime $P(O_3)$ attributable to HO_2-driven NO-to-NO_2 conversion (Fig. 4), higher contributions were observed in the northern YRD, coinciding with elevated NO_x emission rates (approximately 0.4−2.0 mole s^{-1}; Fig. R5). In these regions, the more pronounced influence of HO_2 compared to RO_2 on $P(O_3)$ is primarily associated with markedly higher HO_2 concentrations. OVOCs dominated primary HO_2 production (>90%) in this region, with primary OVOCs alone contributing approximately 20−50% (Fig. 4). In addition, OVOCs contributed approximately 50−98% of primary RO_2 and 40−70% of primary RO_x production, suggesting that OVOCs also play an important role in sustaining HO_2 levels through radical cycling. Taken together, the pronounced influence of HO_2 on $P(O_3)$ in urban regions is likely driven by elevated levels of both primary OVOCs and secondary OVOCs formed from VOC oxidation. Such conditions, characterized by coexisting high emissions of reactive organic gases and NO_x, are conducive to enhanced HO_2 production. We have added a discussion in the revised manuscript as follows:

Lines 311-322: "The dominant role of HO_2-driven oxidation in ozone production was further confirmed in other urban areas of the YRD. During both EP1 and EP2, HO_2 radicals contributed approximately 55−80% of total ozone production in regions with elevated $P(O_3)$ (Figs. 4a, d and S11a, d). These regions, including Shanghai, are strongly affected by anthropogenic emissions, with substantial NO_x emission rates (approximately 0.4−2.0 mole s^{-1}; Fig. S9) and HO_2 concentrations exceeding those of RO_2 radicals (Fig. S11). In these urban areas, primary OVOCs from major sources, such as industrial processes, solvent use, residential sources, and transportation, made substantial contributions to $P(O_3)$ and peroxy radical levels (particularly HO_2), ranging 5−40% and 4−47%, respectively (Figs. S12−S15). In contrast, the RO_2 pathway dominated ozone production in the southern and southwestern parts of the domain,

where high emissions of biogenic VOCs and relatively low emissions of NO_x prevail (Fig. S9). The enhanced role of RO_2 radicals in these regions is attributed to their higher concentrations and comparable reactivities to HO_2 radicals in converting NO to NO_2."

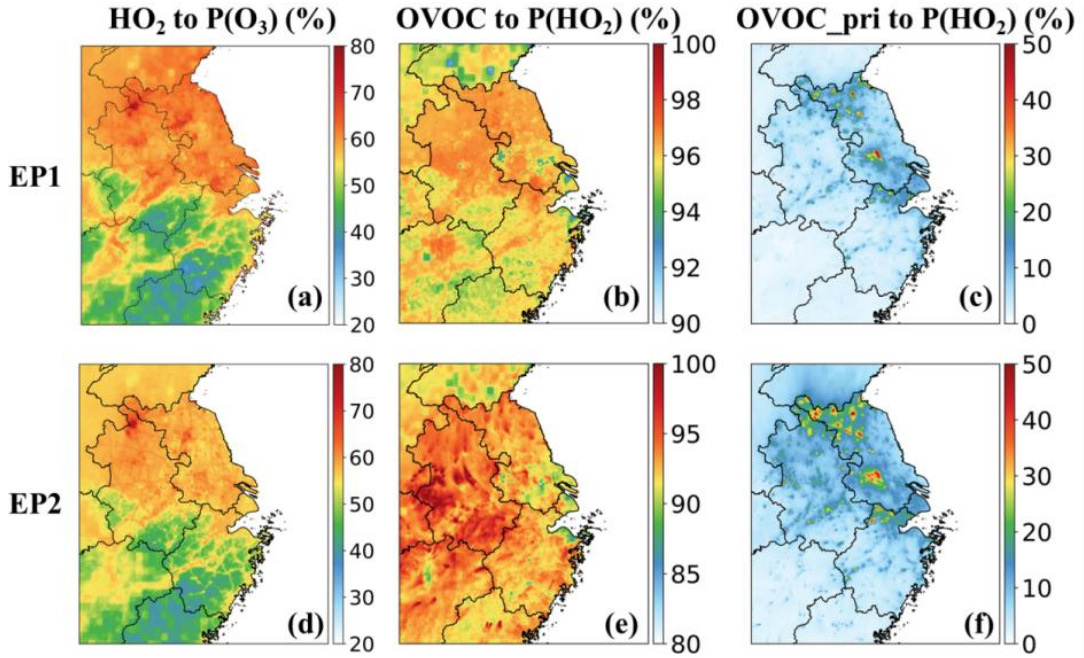

Figure 4. Daytime-averaged contributions of the HO_2 + NO pathway to ozone production rates (a, d), OVOC contributions to primary HO_2 radical production (b, e), and contributions from primary OVOCs (c, f) during the two episodes.

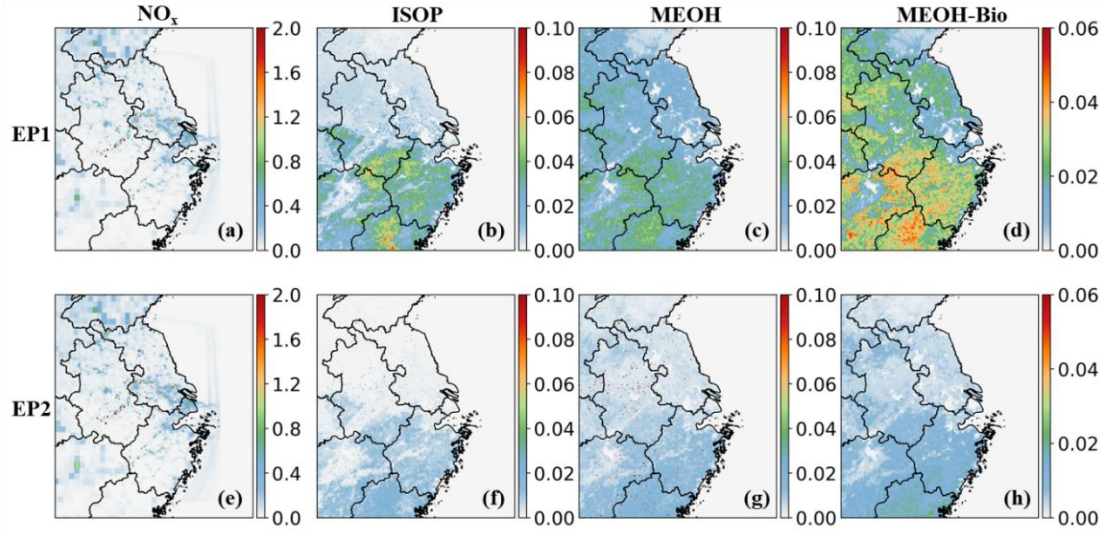

Figure R5. Average emission rates of NO_x, isoprene, MEOH, and biogenic MEOH during EP1 and EP2. Units are mole s^{-1}.

Specific Comments:

Comment: *1. Line 150. The study mentions that emissions of highly volatile OVOCs such as ethanol are significantly affected by temperature, but the current model has not*

fully incorporated temperature-dependent parameterization. It is recommended to supplement the basis for the setting of temperature-related parameters in the existing emission inventory, or provide a sensitivity analysis to verify the degree of temperature's impact on the simulation results.

Response: Thank you for this valuable comment. In the current emission inventory, evaporative emissions (e.g., from solvent use and gasoline evaporation) are not explicitly parameterized as temperature-dependent. To assess the potential impacts, we conducted additional sensitivity simulations by applying temperature-dependent adjustments to solvent use and gasoline evaporative OVOC emissions, following the approach used in our previous study (Qin et al. 2025). The simulated concentrations of OVOCs, including ethanol (ETOH), acetone (ACET), and formaldehyde (HCHO), showed slight decreases during the warm season (EP1) and more pronounced reductions during the cold season (EP2) across the YRD region (Fig. R6).

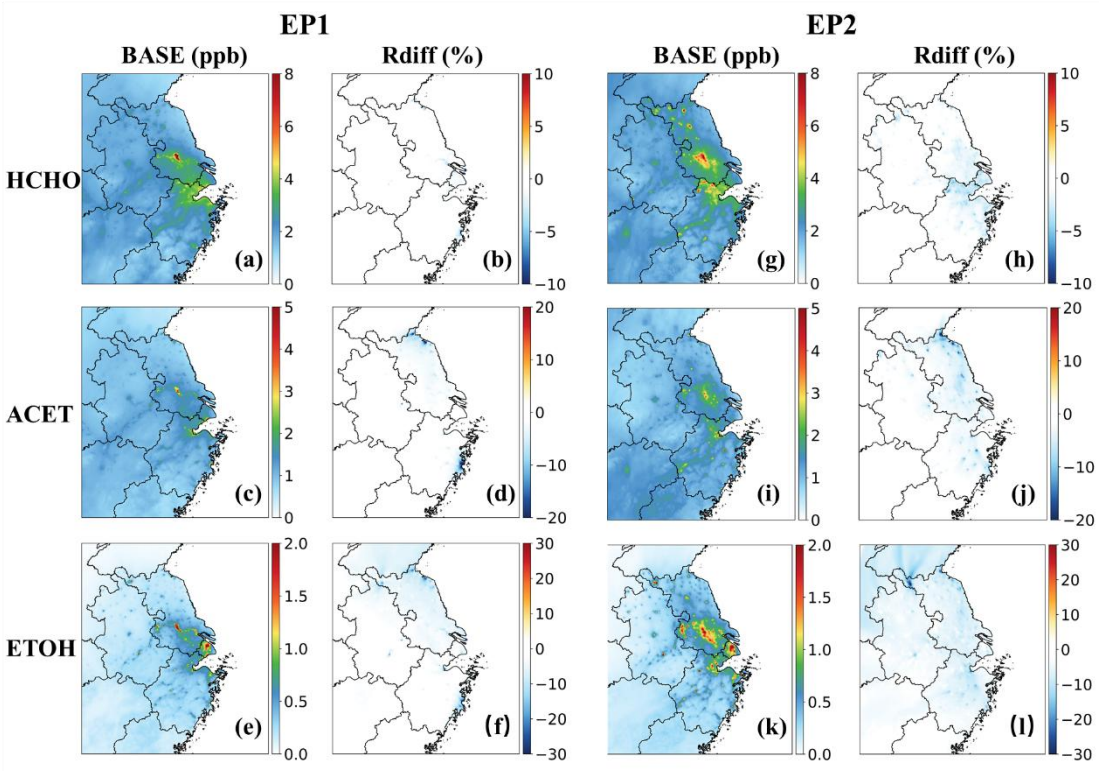

Figure R6. Episode averaged concentrations of HCHO, ACET, and ETOH in the base case (unit: ppb) and the relative changes due to temperature-adjusted evaporative emissions (Rdiff, (tempadj-base)/base %).

This is because the daily maximum surface temperature during both episodes, particularly in regions strongly influenced by anthropogenic emissions, was lower than the reference temperature (25 °C) used to scale evaporative emissions based on temperature-dependent emission factors. We acknowledge that this adjustment approach is still subject to uncertainties, including the choice of reference temperature and potential variability in temperature dependence among different volatile species

due to differences in vapor pressure. A more robust assessment of temperature-dependent evaporative emissions would require species-specific temperature-emission relationships from different sources, which is beyond the scope of the present study. To avoid confusion and potential misinterpretation, we have therefore removed the related discussion on the impacts of temperature-dependent evaporative emissions on OVOC simulations from the revised manuscript.

Comment: *2. Line 170. The model shows consistent underestimation of species such as formic acid and acetic acid, and seasonal differences in the simulation of acetone (ACET). In addition to the uncertainties in the emission inventory and missing secondary formation pathways mentioned in the paper, have the local source impacts of the observation site been considered? It is recommended to supplement a brief description of the pollution source distribution around the site.*

Response: Thank you for this suggestion. The monitoring site is strongly affected by emissions from transportation and solvent use. Correlation analysis for acetic acid with other measured species showed high correlations with ethyl acetate, methyl ethyl ketone (MEK), and toluene (Pearson coefficients of 0.75−0.85, $p < 0.001$) in both periods. These compounds are typically associated with emissions from volatile chemical products (VCPs), consistent with the significant impacts of solvent use at the site. Additionally, strong correlations between acetic acid and biomass burning tracers (e.g., guaiacol and furan compounds and their derivatives) were observed during EP2, indicating an influence of this source on acetic acid at the monitoring site. Inadequate representations of these emissions may lead to biases in the current model.

For ACET, a more pronounced model bias is observed in EP1 (warm season) than in EP2 (cold season). As biogenic emissions are an important source of ACET, this bias may be partially attributed to underestimated biogenic emissions from urban green spaces near the monitoring site as also reflected by the model biases in isoprene. We have incorporated the related discussion into the manuscript in Lines 199-205:

"During EP2, acetic acid exhibited strong correlations with biomass burning tracers, such as guaiacol and furan compounds and their derivatives (Pearson coefficients > 0.80, $p < 0.001$). In addition, acetic acid showed consistently high correlations with ethyl acetate, methyl ethyl ketone (MEK), and toluene (Pearson coefficients of 0.75−0.85, $p < 0.001$) in both periods, species that are commonly associated with emissions from volatile chemical products (VCPs) (Wang et al., 2024b; McDonald et al., 2018). The underestimation of emissions from these sources likely contributes to the low bias in simulated acetic acid concentrations."

Lines 234-237: "Model performance for ACET varied seasonally, with good agreement in EP2 but significant underestimation in EP1. Since biogenic sources of acetone are

important (Lyu et al., 2024; Hu et al., 2013), the larger discrepancy observed in the warm season may be partially due to the model's inadequate representation of urban green vegetation (Maison et al., 2024; Ma et al., 2022)."

A description of the local emission impacts on the observation site is provided in Lines 187-189:
"The monitoring site is located in a typical urban environment characterized by dense commercial and residential buildings and heavy traffic, with strong influences from transportation and solvent use emissions (Liu et al., 2019; Liu et al., 2021)."

Comment: *3. Section 3.2. Since RO_2, HO_2, and OH can interconvert through the RO_x radical cycle, and the contribution of RO_2 to $P(O_3)$ cannot be ignored, especially in northern Zhejiang Province. It is requested to provide the contributions of OVOCs to primary RO_x radicals and RO_2 radicals. Which OVOCs are relatively important in this process?*

Response: Thank you for this insightful comment. We agree with the reviewer that RO_2, HO_2, and OH radicals are closely correlated and interconvert through radical chemistry. Therefore, we focus on primary RO_2, HO_2, and RO_x production, which are defined as those generated only as products in the reactions, such as photolysis of OVOCs, O_3, HONO, and ozonolysis of OVOCs and VOCs (Figs. 3, 4, and S16). Primary radicals initiate atmospheric radical chemistry and trigger radical chain reactions, ultimately leading to ozone accumulation. By focusing on the contribution of OVOCs to primary radical production, we provide a clearer and more robust assessment of their role in ozone formation. The results show that OVOCs contribute 63.96% (66.49%) and 95.31% (97.03%) of primary RO_2 and HO_2 at the monitoring site during clean (polluted) periods. Formaldehyde (HCHO), photoreactive monounsaturated dicarbonyls from aromatic fragmentation (AFG1), methylglyoxal (MGLY), and glyoxal (GLY) are the major contributors to HO_2 radical. A significant fraction of RO_2 radicals is produced by biacetyl (BACL), AFG1, and MGLY. For RO_x radicals, 50.18% and 43.17% are attributed to OVOC photooxidation under clean and polluted conditions. At the regional scale, the contributions of OVOCs to primary HO_2, RO_2, and RO_x radicals can reach approximately 90−98%, 50−98%, and 40−70%, respectively. These findings indicate a dominant role of OVOCs in radical production in the YRD. We have revised the manuscript to include a discussion on the role of OVOCs on primary HO_2, RO_2, and RO_x production in Section 3.2 (now Section 3.3).

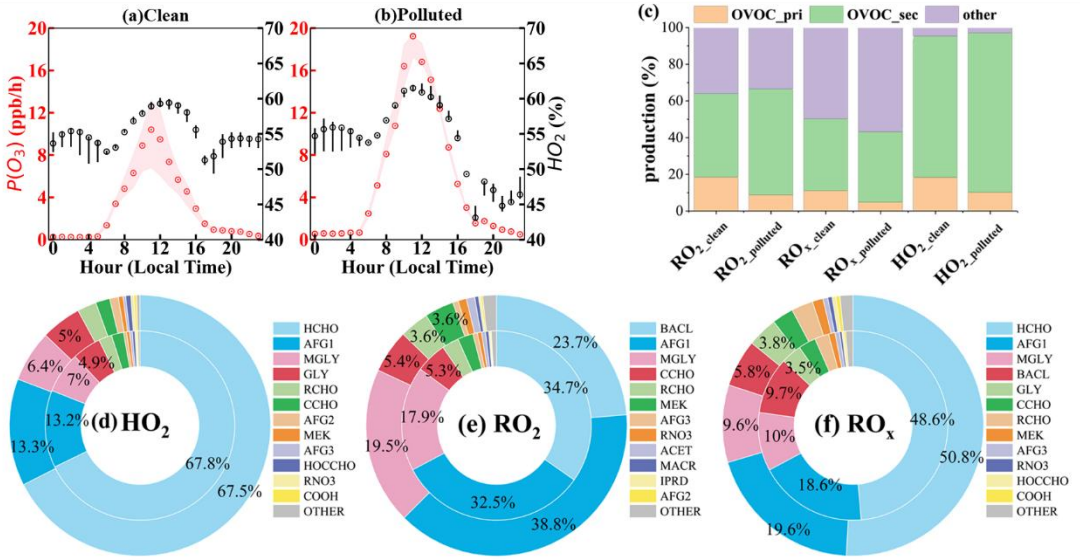

Figure 3. Diurnal variations of ozone production rates (a, b) and contributions of major sources (c) and individual OVOC species (d-f) to daytime primary HO_2, RO_2, and RO_x production under clean and polluted conditions at SAES in Shanghai. In panels (a) and (b), red and black circles represent the median $P(O_3)$ and the contribution of the HO_2 + NO pathway, respectively. The shaded areas and black error bars denote the interquartile ranges. In panel (c), "OVOC_pri" and "OVOC_sec" denote contributions from primary and secondary OVOCs, respectively. Panels (d-f) show the fractional contributions of individual OVOC species to total OVOC-derived primary radical productions during clean (inner ring) and polluted (outer ring) periods.

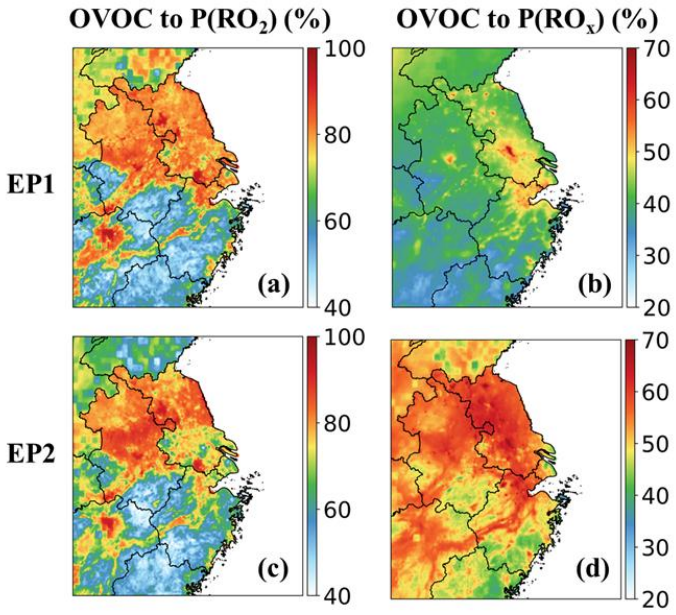

Figure S16. Contributions of OVOCs to the daytime primary RO_2 and RO_x radical production during EP1 and EP2.

Comment: *4. Section 3.3. When evaluating the sensitivity of ozone formation to OVOCs, explain why the emission reductions of some OVOCs lead to a nonlinear*

response of slight increases in ozone concentration, and whether this is related to the regional NO_x concentration levels? Will the experimental setup change NO_X? It is recommended to add relevant discussions in this section.

Response: Thank you for pointing out this phenomenon that requires an in-depth explanation. The High-Order Decoupled Direct Method (HDDM) calculates the spatially and temporally varying sensitivity coefficients of ozone changes to small perturbations in precursor emissions, i.e., the partial derivatives between the two. It can deal with the non-linear relationship between ozone and precursors by utilizing second-order (and higher) sensitivities, and compute ozone sensitivities to multiple precursors at once. In the current study, the first- and second-order sensitivity coefficients of each OVOC and VOC species are used to estimate ozone sensitivities to their emission changes, without altering NO_x emissions or concentrations.

The slight increase in ozone concentration observed in the simulation of emission reductions for certain OVOCs is likely related to their mechanisms in regulating NO_x and radical cycling. During the daytime, photooxidation of some aldehydes and ketones, such as acetaldehyde (CCHO), aromatic aldehydes (BALD), lumped C_3+ aldehydes (RCHO), and acrolein (ACRO), produces peroxyacyl radicals that can react with NO_2 to produce NO_x reservoir species, such as PAN and analogues. Reducing their emissions may therefore decrease PAN formation, allowing more NO_2 to remain available for NO_x cycling and thereby enhancing ozone production. At the same time, the photooxidation of CCHO, RCHO, and ACRO also produces other RO_2 and HO_2 radicals that promote NO-to-NO_2 conversion, implying that reductions in these OVOCs can partially suppress ozone formation by limiting peroxy radical production. Because the emission rates of these OVOCs, as well as the types and yields of radicals produced from their oxidation, vary substantially across the YRD, the net ozone response to their emission reductions exhibits spatial heterogeneity. Similarly, the products of CRES oxidation can either react with NO_2 to form relatively stable products or promote RO_2 and HO_2 productions, leading to regional differences in ozone responses to CRES emission reductions. We have added relevant discussions in the revised manuscript as follows:

Lines 404-410: "Notably, emission reductions of certain OVOCs (e.g., CCHO, RCHO, ACRO, and CRES) can lead to spatially divergent ozone responses, with both increases and decreases in the YRD. This likely arises from differences in the radical pathways associated with OVOC photooxidation: some pathways involve reactions with NO_2 to form relatively stable NO_x reservoir species, whereas others promote NO-to-NO_2 conversion. The competition between these pathways varies regionally with the abundances of OVOCs and NO_x, resulting in spatial heterogeneity in ozone sensitivities."

Comment: *5. Line 127. Since PTR can only measure the total molecular signal, how to process its measured data to distinguish the concentration of specific OVOCs? Alcohols produce fragments during proton transfer reactions, such as (C2H6OH+H+ → C2H4H++H2O). How to handle the concentration of alcohols measured by PTR?*

How is the quantification of OVOCs done? Can you supplement the comparison of two MSs?

Response: Thank you for this important comment that helps enhance the validity of OVOC measurements. As noted by the reviewer, proton-transfer-reaction time-of-flight mass spectrometry (PTR-ToF-MS) is capable of resolving isobaric ions but remains intrinsically limited to molecular-level characterization and cannot unambiguously distinguish isomers. In this study, the molecular formula for individual mass spectral peaks was first constrained by jointly applying the elemental composition tool implemented in the Tofware software package v3.2.3 (Tofwerk Inc.), the PTR-MS spectral library (Pagonis et al., 2019), and the PubChem database. Based on these plausible molecular formulae, tentative compound identifications were further inferred by integrating previously reported source-specific emission profiles from the literature. For species quantification, sensitivities for species with authentic standards were determined through calibration using multi-gradient known concentrations of given VOCs. For identified species lacking standards, their theoretical sensitivities were estimated based on the correlations with kinetic rate constants of VOCs (Sekimoto et al., 2017). This approach has been successfully employed to identify reactive organic gases emitted from residential combustion in the YRD (Gao et al., 2022; 2023).

Alcohol compounds are prone to fragmentation during proton transfer reactions, such that the primary ion typically accounts for ~80% of the total ion signal, resulting in an approximate 20% underestimation of their concentrations. In the current study, small alcohols such as methanol and ethanol were detected using an online gas chromatography system equipped with a mass spectrometer and a flame ionization detector (GC-MS/FID). The results for major aromatic hydrocarbons and carbonyl compounds measured by PTR-QiTOF and GC-MS/FID showed good agreement, as illustrated in Fig. S5 of Gao et al (2022).

We have revised the manuscript with detailed information on the treatment of PTR-QiTOF measurements and comparison between PTR-QiTOF and GC-MS/FID as follows:

Lines 148-160: "High time-resolution measurements of 77 OVOCs, including 14 aldehydes and ketones, 23 organic acids and esters, 10 furan compounds, and 30 oxygenated aromatic compounds, were recorded at a 10s interval using a Proton

Transfer Reaction-Quadruple interface Time-of-Flight Mass Spectrometer (PTR-QiTOF) at the Shanghai Academy of Environmental Sciences (SAES). Species were identified by jointly applying the Tofware software package v3.2.3 (Tofwerk Inc.), the proton transfer reaction mass spectrometry (PTR-MS) spectral library (Pagonis et al., 2019), the PubChem database, and source-specific emission profiles reported in literature (Hatch et al., 2017; Koss et al., 2018; Stockwell et al., 2021; Tanzer-Gruener et al., 2022; Coggon et al., 2021). Sensitivities for species with authentic standards were determined through calibration using multi-gradient known concentrations of given VOCs. For identified species lacking standards, their theoretical sensitivities were estimated based on correlations with kinetic rate constants of VOCs (Sekimoto et al., 2017). The raw data were screened to remove outliers (values below background levels) and missing data, and then averaged to hourly means."

Lines 161-165: "In addition, C_2–C_{12} hydrocarbons, C_2–C_5 carbonyls, and C_1–C_4 alcohols were measured using an online gas chromatography system equipped with a mass spectrometer and a flame ionization detector (GC-MS/FID, TH-300, Wuhan Tianhong Instruments, China) at an hourly resolution. For major aromatic hydrocarbons and carbonyl compounds, good agreement between measurements by PTR-QiTOF and GC-MS/FID was observed (Gao et al., 2022)."

Comment: *6. With reference to Table S6, could the contribution ratios of different sources to each OVOC in EP1 and EP2 be provided separately?*
Response: Thank you for this suggestion. The current study mainly focuses on the implementation of a newly developed emission inventory to improve the simulations of OVOCs and assess their roles in ozone formation, particularly for that of primary OVOCs. The development of the inventory, including the source profiles of all the pollutants emitted from anthropogenic sectors, will be detailed in another manuscript.

Comment: *7. It is recommended that the fonts in the figures and tables be consistent.*
Response: We have reviewed and standardized the fonts across all figures (primarily using Times New Roman), ensuring consistency in size and style to meet the journal's figure formatting requirements.

Comment: *8. Fig. 1 (2) b, (3) c, and (4) d. Why do the diurnal variations of model-simulated Isoprene and its oxidation products MVK and MACR exhibit a bimodal distribution, which is opposite to the observed diurnal characteristics? Since isoprene is a typical biogenic VOC, it is reasonable for its concentration to be high during the daytime, while the model-simulated values are close to zero at noon.*
Response: The model bias in the noon peak of isoprene is likely attributed to the underestimation in biogenic emissions from urban green spaces, which further affects

the simulation of MVK and MACR. We have added a related discussion in the revised manuscript:

Lines 238-242: "Notably, biases in OVOC concentrations are influenced by those of their precursors. For example, model biases in methacrolein (MACR) and methyl vinyl ketone (MVK) exhibited similar temporal patterns to those of isoprene (ISOP), reflecting their common origin via isoprene oxidation. The model failed to reproduce the peak noon concentration of isoprene, likely due to the underestimated biogenic emissions from urban green spaces."

Comment: *9. Line 44. Delete "and thus deviate from observations".*

Response: The phrase has been removed.

References

Gao, Y., Wang, H., Yuan, L., Jing, S., Yuan, B., Shen, G., Zhu, L., Koss, A., Li, Y., Wang, Q., Huang, D. D., Zhu, S., Tao, S., Lou, S., and Huang, C.: Measurement report: Underestimated reactive organic gases from residential combustion – insights from a near-complete speciation, Atmos. Chem. Phys., 23, 6633-6646, 10.5194/acp-23-6633-2023, 2023.

Gao, Y. Q., Wang, H. L., Liu, Y., Zhang, X., Jing, S. A., Peng, Y. R., Huang, D. D., Li, X., Chen, S. Y., Lou, S. R., Li, Y. J., and Huang, C.: Unexpected High Contribution of Residential Biomass Burning to Non-Methane Organic Gases (NMOGs) in the Yangtze River Delta Region of China, J. Geophys. Res. Atmos., 127, 14, 10.1029/2021jd035050, 2022.

Pagonis, D., Sekimoto, K., and de Gouw, J.: A Library of Proton-Transfer Reactions of H3O+ Ions Used for Trace Gas Detection, Journal of the American Society for Mass Spectrometry, 30, 1330-1335, 10.1007/s13361-019-02209-3, 2019.

Qin, M. M., She, Y. L., Wang, M., Wang, H. L., Chang, Y. H., Tan, Z. F., An, J. Y., Huang, J., Yuan, Z. B., Lu, J., Wang, Q., Liu, C., Liu, Z. X., Xie, X. D., Li, J. Y., Liao, H., Pye, H. O. T., Huang, C., Guo, S., Hu, M., Zhang, Y. H., Jacob, D. J., and Hu, J. L.: Increased urban ozone in heatwaves due to temperature-induced emissions of anthropogenic volatile organic compounds, Nat. Geosci, 15, 10.1038/s41561-024-01608-w, 2025.

Sekimoto, K., Li, S.-M., Yuan, B., Koss, A., Coggon, M., Warneke, C., and de Gouw, J.: Calculation of the sensitivity of proton-transfer-reaction mass spectrometry (PTR-MS) for organic trace gases using molecular properties, International Journal of Mass Spectrometry, 421, 71-94, https://doi.org/10.1016/j.ijms.2017.04.006, 2017.

Response to Reviewer #4

Overview:

Comment: *The manuscript presents a timely and valuable investigation into the role of oxygenated volatile organic compounds (OVOCs) in atmospheric chemistry and regional air quality, with a specific focus on the Yangtze River Delta (YRD) region. OVOCs remain a major source of uncertainty in air quality modeling due to poorly constrained emissions, and this study addresses an important gap by incorporating updated, source-resolved OVOC emission profiles into the CMAQ model. The topic is highly relevant to both atmospheric chemistry research and practical air quality management, particularly in rapidly urbanizing and polluted regions such as the YRD. However, several aspects of the manuscript require revision before it can be deemed acceptable for publication in ACP.*

Response: We thank the reviewer for the constructive and positive feedback on our study. The comments have been very helpful in improving the clarity and overall quality of the manuscript. In response to the reviewer's suggestions, we have: (1) provided a detailed description of the methodology for constructing source profiles; (2) evaluated the impact of temporary control measures during the 2019 China International Import Expo (CIIE); and (3) made revisions to improve the accuracy and clarity of the text and figures. Detailed responses to each comment are provided below. The reviewer's comments are shown in black italics, our responses are in blue, and the corresponding revisions in the manuscript are highlighted in red.

Comments:

Comment: *1. Section 2.1: While the paper states that "source-resolved OVOC profiles derived from measurements and literature" were used, additional details on how these profiles were constructed would enhance reproducibility and allow readers to assess potential uncertainties.*

Response: Thank you for the valuable suggestion. Source profiles of the 2019YRD inventory were derived based on the 2017YRD inventory (An et al., 2021), with updates for diesel vehicles, industrial processes, biomass burning, and gasoline vehicles. Profiles of diesel vehicles, industrial processes, and biomass burning were obtained based on 160 source-resolved measurements. For diesel vehicles, twenty in-use heavy-duty vehicles from five major brands were tested, encompassing China VI (n=6), China V (n=10), and China IV (n=4) emission standards. For industrial emissions, a total of 84 samples were collected from priority sectors, including petrochemical industries, chemical raw material production, and other chemical production sectors such as plywood production, coking, pesticides production, ink production, and rubber production. For residential biomass burning, 23 samples of the combustion of four

representative biomass fuels (wood, corncob, bean straw, and corn straw) and two common coal types (anthracite and briquette coal) were collected from the stack nozzles of household stoves. For the gasoline vehicle source, the VOC (including OVOCs) profiles from published literature (Wang et al., 2022a; Huang et al., 2024) were used. A two-step process was then employed to obtain the profile of each source category:

(1) Sub-category Averaging: To minimize the influence of individual sample variability, measurements were averaged to derive stable, representative profiles for each sub-category. For example, diesel vehicle emissions were classified according to China VI, China V, and China IV emission standards, respectively. For industrial processes, representative profiles were derived according to specific industrial stages, raw materials, products, and fuel types. Similarly, for biomass burning emissions, fuel-specific profiles were established.
(2) Weighted Integration: The final integrated source profiles were synthesized by weighting the sub-category profiles according to their respective total VOC emission contributions in the study region.

We have revised the manuscript to reflect these details in Lines 116-134 as follows:
"The VOC composition of emissions from diesel vehicles, industrial processes, and residential biomass burning was characterized based on 160 localized, source-resolved measurements conducted in China. Specifically, twenty in-use heavy-duty diesel vehicles from five major brands were tested, encompassing China VI (n=6), China V (n=10), and China IV (n=4) emission standards. For industrial emissions, a total of 84 samples were collected from priority sectors, including petrochemical industries, chemical raw material production, and other chemical production sectors such as plywood production, coking, pesticides production, ink production, and rubber production. For residential biomass burning, 23 samples of the combustion of four representative biomass fuels (wood, corncob, bean straw, and corn straw) and two common coal types (anthracite and briquette coal) were collected from the stack nozzles of household stoves. Details of the sampling protocols and analytical procedures can be found in a previous study (Gao et al., 2023). VOC profiles for other sources, such as gasoline vehicles, were based on published literature (Wang et al., 2022a; Huang et al., 2024). To develop representative source profiles, a two-step aggregation method was employed. First, sub-category average profiles were derived by averaging individual samples within each specific emission standard, industrial stage, and types of raw materials, products, and fuels. Second, the integrated source profiles were synthesized by weighting these sub-category profiles according to their corresponding total VOC emissions. This method aligns with the national technical guidelines for integrated air pollutant emission inventories (Ministry of Ecology and Environment, 2024)."

Comment: *2. Section 3.1: The authors attribute the overestimation of ethanol in EP2 to the model's omission of temporary emission restrictions during and before the 2019 China International Import Expo (CIIE). To better evaluate the impact of these restrictions, could you provide model results excluding the CIIE period (e.g., by removing those days from the evaluation dataset)? This would help clarify how much of the bias is directly linked to unaccounted emission reductions and improve confidence in attributing the overestimation to this specific event.*

Response: Thank you for the insightful comment. After excluding data from the CIIE period, the observed concentrations of traditional VOCs and OVOCs, such as acetone (ACET), acrolein (ACRO), methyl ethyl ketone (MEK), and ethanol (ETOH), increased. The model performance for most species has been improved, particularly for alkenes, aromatic hydrocarbons, and most OVOCs (Table R1). For ETOH, the normalized mean bias (NMB) and normalized mean error (NME) decrease from 1.67 to -0.084 and from 2.45 to 0.80, respectively. As the temporary emission restrictions applied to major cities in the surrounding area of Shanghai and on the pollution transport pathway in Anhui and Jiangsu Provinces, all data during the CIIE period have been excluded from analysis to reduce potential influences from the temporary emission restrictions.

Table R1. Comparison of observed average concentrations of OVOCs and their VOC precursors (ppb), normalized mean bias (NMB), and normalized mean error (NME) during EP2 at the Shanghai monitoring site. Values outside and inside parentheses represent results with the CIIE period excluded and included, respectively.

Species	Obs	NMB	NME	Species	Obs	NMB	NME
HCHO	2.58 (2.75)	-0.21 (-0.29)	0.32 (0.36)	**OLE1**	0.14 (0.14)	3.31 (3.70)	3.31 (3.70)
CCHO	0.56 (0.60)	0.64 (0.48)	0.74 (0.63)	**OLE2**	0.28 (0.27)	1.71 (2.16)	1.77 (2.24)
ACRO	0.053 (0.048)	1.75 (1.81)	1.81 (1.87)	**BDE13**	0.011 (0.011)	8.8 (10.5)	8.8 (10.5)
ACET	1.89 (1.63)	-0.19 (-0.031)	0.43 (0.51)	**ACYE**	1.35 (1.38)	-0.25 (-0.21)	0.54 (0.53)
MACR	0.018 (0.021)	0.79 (0.33)	1.06 (0.82)	**ALK1**	6.83 (6.70)	-0.7 (-0.68)	0.7 (0.68)
MEK	0.64 (0.54)	0.17 (0.41)	0.59 (0.66)	**ALK2**	4.22 (4.17)	-0.63 (-0.63)	0.65 (0.64)
MVK	0.026 (0.034)	1.03 (0.64)	1.17 (1.00)	**ALK3**	2.62 (2.60)	-0.27 (-0.22)	0.47 (0.51)
RCHO	0.36	0.11	0.35	**ALK4**	2.42	0.48	0.69

	(0.44)	(-0.072)	(0.35)		(2.30)	(0.70)	(0.89)
ETOH	3.24 (1.33)	-0.084 (1.67)	0.80 (2.45)	**ALK5**	1.34 (0.98)	0.26 (0.98)	0.62 (1.21)
HCOOH	1.95 (3.57)	-0.96 (-0.98)	0.99 (0.98)	**ARO1**	0.45 (0.41)	1.3 (1.63)	1.4 (1.67)
CCOOH	2.59 (2.66)	-0.75 (-0.78)	0.76 (0.79)	**ARO2MN**	0.32 (0.27)	1.45 (2.02)	1.54 (2.07)
CRES	0.41 (0.50)	-0.51 (-0.67)	0.72 (0.78)	**BENZ**	0.47 (0.45)	0.73 (0.87)	0.8 (0.97)
PAN	0.61 (0.63)	-0.35 (-0.42)	0.40 (0.5)	**TOLU**	1.11 (1.05)	0.16 (0.19)	0.55 (0.72)
ETHE	1.96 (1.75)	0.16 (0.39)	0.55 (0.82)	**MPXYL**	0.63 (0.53)	1.48 (2.21)	1.58 (2.29)
PROP	0.58 (0.44)	1.39 (1.82)	1.57 (1.93)	**OXYL**	0.25 (0.22)	1.29 (1.90)	1.41 (2.00)
ISOP	0.019 (0.020)	0.23 (0.31)	0.79 (0.96)	**B124**	0.053 (0.046)	1.77 (2.39)	1.80 (2.41)

Comment: *3. Figure S7: Observational data indicate that ethanol concentrations were markedly lower during the CIIE period. Given that approximately 30−70% of total OVOCs originated from primary emissions, did other OVOC species such as HCHO show a similar decreasing trend during the same period?*

Response: Thank you for this valuable comment. We compared the concentrations of key OVOC species and traditional VOCs (i.e., alkanes, alkenes, and aromatic hydrocarbons) during the EP2 (Table R1). Most alkanes, alkenes, and aromatic hydrocarbons increased after excluding data from the CIIE period. Among OVOC species, ACET, ACRO, MEK, and ETOH increased, while HCHO, HCOOH, MVK, and RCHO decreased. The distinct responses among OVOCs may be attributed to differences in the relative contributions of their direct emissions and secondary formation from precursor oxidation production. In addition, variations in source-specific control strategies may lead to diverse changes in OVOC concentrations. To minimize potential impacts of temporary emission restrictions, both observed and modeled data during the CIIE period were excluded from the analysis in the revised manuscript.

Comment: *4. Line 171: In the manuscript, the authors state a temperature difference as "2.5 ℃ (16.8%) higher". Expressing a temperature change as a percentage can be misleading because the result depends on the choice of reference temperature and*

temperature scale (°C vs. K). For example, the same ΔT corresponds to ~16.8% if referenced to 14.9 °C, but only ~0.87% if referenced to the absolute temperature in Kelvin.

Response: Thank you for pointing this out. We agree with the reviewer that relative temperature changes can differ substantially depending on whether they are calculated using Celsius and Kelvin, which may introduce biases in the interpretation of temperature sensitivities.

Following suggestions from other reviewers, we have conducted additional sensitivity simulations by applying temperature-dependent adjustments to solvent use and gasoline evaporative OVOC emissions, following the approach used in our previous study (Qin et al. 2025). Compared with the original results, a general decreasing trend was found, particularly in the colder episode (EP2) (Fig. R1). This is because the daily maximum surface temperature during both episodes in regions strongly influenced by anthropogenic emissions remained below the reference temperature (25 °C) used to scale evaporative emissions based on temperature-dependent emission factors. We acknowledge that this adjustment approach is still subject to uncertainties, including the choice of reference temperature and potential variability in temperature dependence among different volatile species due to differences in vapor pressure. A more robust assessment of temperature-dependent evaporative emissions would require species-specific temperature-emission relationships from different sources, which is beyond the scope of the present study. To avoid confusion and potential misinterpretation, we have therefore removed the related discussion on the impacts of temperature-dependent evaporative emissions on OVOC simulations from the revised manuscript.

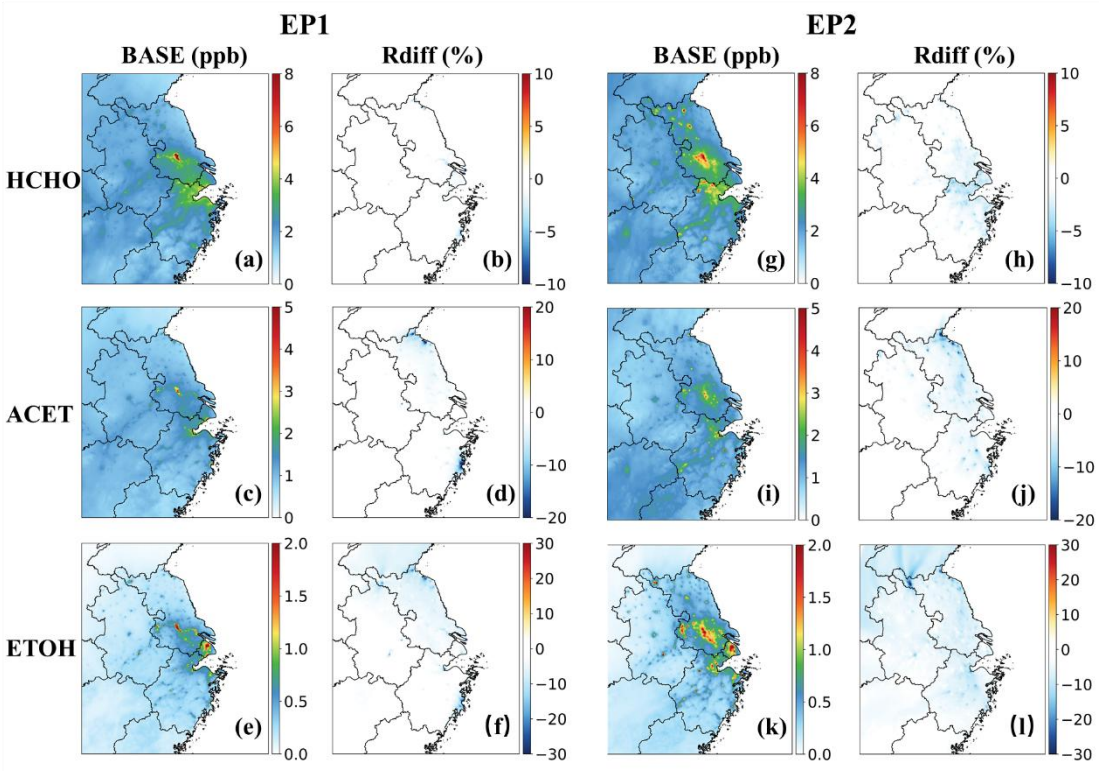

Figure R1. Episode averaged concentrations of HCHO, ACET, and ETOH in the base case (unit: ppb) and the relative changes due to temperature-adjusted evaporative emissions (Rdiff, (tempadj-base)/base %).

Comment: *5. Lines 213-214: The authors state that "Most OVOCs exhibited higher concentrations in EP2 than in EP1, except for MEOH", but this is not entirely consistent with the observational results, at least based on the comparison between Figs 2 and S6. Considering the short-term emission reductions during the CIIE period, the substantial decrease in anthropogenic OVOC emissions during EP2 should lead to reduced concentrations for some OVOCs.*

Response: Thank you for pointing this out. The different seasonal trends between modeled and observed OVOCs may likely be attributed to several reasons. Firstly, the temporary emission control during CIIE was not considered in model simulations, resulting in higher predicted OVOC concentrations during EP2. To assess this impact, data from the CIIE period were excluded. Although the observed concentrations of several OVOC species increased, most OVOCs, such as carbonyl species, remained higher during EP1 than in EP2 (Table S5), contrary to model predictions. This suggests that the discrepancy between modeled and observed seasonal OVOC trends is likely due to model biases. As shown in Table S5, most OVOCs are underestimated, with the biases being particularly pronounced during EP1. However, OVOC trends in other parts of the YRD may differ from those in Shanghai, due to the complexity of industrial processes in this region, a primary emission source of OVOCs and their precursors. Additional long-term observations at other sites would be helpful for a better

understanding of the seasonal variability of OVOCs in the YRD. To improve the clarity of the manuscript, the text has been revised as follows:
Lines 256-258: "In contrast to observations in Shanghai, the model predicted higher concentrations of most OVOCs in EP2 than in EP1 across the YRD, likely due to biases in the model representation of OVOCs (Table S5)."

A discussion on the modeled OVOC seasonal trends has been added in Section 4 as follows:
Lines 453-454: "The underestimation of OVOCs may result in biased predictions of their seasonal variability."

Comment: *6. Line 341: "facilitate" should be "facilitates".*
Response: The word has been revised.

Comment: *7. The authors mention that "In the HO2 pool, approximately 16.6% was newly generated, with OVOC photolysis being the dominant source (94.1%)". However, the presentation in Fig. 2c is somewhat misleading. It is recommended that the authors further clarify the relative proportions of "newly generated" HO2 and "primary" HO2 in Figure 2.*
Response: Thank you for this valuable comment. As HO_2, RO_2, and OH radicals are closely coupled and mutually interdependent, we now focus on primary radical production from photolysis of OVOCs, O_3, HONO, and ozonolysis of OVOCs and unsaturated VOCs, in which radicals are generated solely as products. Contributions from radical interconversion and cycling are therefore not included. Primary radicals initiate atmospheric radical chemistry and trigger radical chain reactions, ultimately leading to ozone accumulation. By focusing on the contribution of OVOCs to primary radical production, we provide a clearer and more robust assessment of their role in ozone formation. Overall, OVOC photooxidation is the dominant source of primary HO_2 across the YRD, accounting for more than 90% (Fig. 4). The figures and manuscript have been updated accordingly.

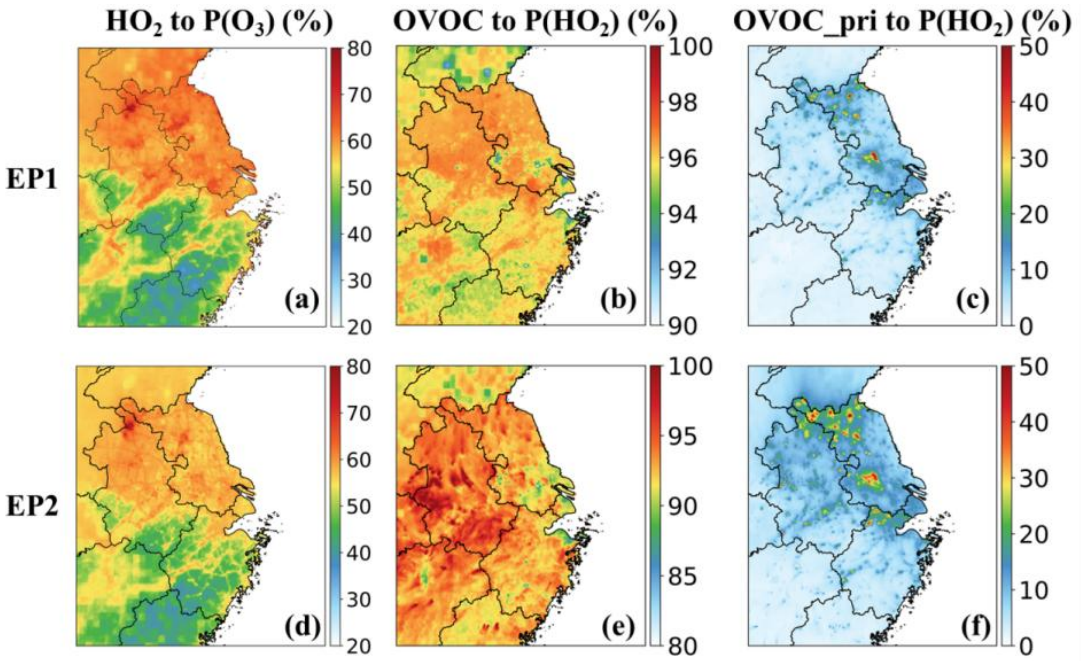

Figure 4. Daytime-averaged contributions of the HO_2 + NO pathway to ozone production rates (a, d), OVOC contributions to primary HO_2 radical production (b, e), and contributions from primary OVOCs (c, f) during the two episodes.

Reference

Qin, M. M., She, Y. L., Wang, M., Wang, H. L., Chang, Y. H., Tan, Z. F., An, J. Y., Huang, J., Yuan, Z. B., Lu, J., Wang, Q., Liu, C., Liu, Z. X., Xie, X. D., Li, J. Y., Liao, H., Pye, H. O. T., Huang, C., Guo, S., Hu, M., Zhang, Y. H., Jacob, D. J., and Hu, J. L.: Increased urban ozone in heatwaves due to temperature-induced emissions of anthropogenic volatile organic compounds, Nat. Geosci, 15, 10.1038/s41561-024-01608-w, 2025.